Asian Journal of Chemistry; Vol. 38, No. 1 (2026), 35-44
ASIAN JOURNAL OF CHEMISTRY
https://doi.org/10.14233/ajchem.2026.34730

Design and Synthesis of Fused 1,2,3-Triazolo-Pyrano-Quinazoline Using Copper(I) Catalysis: *In silico* Molecular Docking, *in vitro* Tyrosine Inhibition and ADMET Studies

SAIDI REDDY MODUGU[1], GOUTHAMI DASARI[2], SATHEESH KUMAR NUKALA[3,*], ASHOK KUMAR BAPURAM[4], RAJU MANNOORI[1] and BANDARI SRINIVAS[1,*]

[1]Department of Chemistry, Chaitanya Deemed to be University, Himayathnagar, Moinabad, Hyderabad-500075, India
[2]Department of Chemistry, J.B. Institute of Engineering & Technology, Yenkapally (V), Moinabad (M), Ranga Reddy (D), Hyderabad-500075, India
[3]Department of Chemistry, Government Junior College, Mustabad, Rajanna Sircilla-505404, India
[4]Department of Chemistry, Guru Nanak Institutions Technical Campus (GNITC B-Tech-I), Ibrahimpatnam, Ranga Reddy, Hyderabad-501506 India

*Corresponding author: E-mail: bandarisrinivas2005@gmail.com

Received: 20 August 2025 *Accepted*: 24 October 2025 *Published online*: 31 December 2025 AJC-22219

In this work, the synthesis of novel 1,2,3-triazolo-pyrano-quinazoline conjugates (**6a-n**) using well-known copper-catalyzed CuAAC and C-H arylation cascade reactions is carried out. The anticancer activity of these conjugates was evaluated against two human cancer cell lines, MCF-7 and HepG-2. The results showed that conjugate **6e** exhibited more potent activity compared to the standard drug erlotinib, while compounds **6b**, **6d** and **6f** displayed slightly lower activity compared to the standard drug. These four potent compounds (**6b**, **6d, 6e** and **6f**) were assessed in a cell survival assay employing the normal breast cell line MCF-10A. None of them showed significant cytotoxicity, with IC_{50} values larger than 98.20 µM. *In vitro* tyrosine kinase EGFR inhibitory of four potent compounds were evaluated and results indicate that compound **6e** exhibited higher EGFR inhibitory activity compared to the standard drug erlotinib. On the other hand, compounds **6b** and **6f** displayed lower activity compared to both the standard drug and compound **6e**. Furthermore, the molecular docking studies were also performed on four potent conjugates and the results showed that these conjugates had more EGFR-binding interactions as compared to the standard drug erlotinib. Moreover, the *in silico* pharmacokinetic outline of the potent conjugates **6b**, **6d, 6e** and **6f** was estimated by using SWISS/ADME and pkCSM and all the four conjugates followed Lipinski rule of five, Ghose, Veber, Egan and Muegge rules without any deviation.

Keywords: 1,2,3-Triazolo-pyrano-quinazoline conjugates, Anticancer activity, Molecular docking studies, Pharmacokinetic profile.

INTRODUCTION

Cancer is one of the most serious health problems and the second leading cause of life-threatening conditions after cardiac illness [1]. Furthermore, the mortality rate reached 9.6 million deaths in 2018 [2]. Currently available anticancer drugs have several severe side effects, including non-selectivity and haematological, gastrointestinal, hepatic, nervous system, cardiac and pulmonary toxicities. There is an urgent need to design new anticancer drugs with minimal side effects or modify existing drug structures to overcome their adverse effects [3,4].

1,2,3-Triazole is one of the important classes of nitrogen atom-containing heterocycles. This heterocycle has the capability to form various non-covalent interactions, such as hydrophobic interactions, hydrogen bonds, van der Waals forces and dipole-dipole bonds, with different biological targets. 1,2,3-Triazoles and their derivatives have shown different pharmaceutical activities, including anticancer [5,6], antiviral [7,8], antibacterial [9,10], antifungal [11,12] and antitubercular [13,14] and antimalarial [15,16]. Furthermore, several compounds comprising 1,2,3-triazoles, including cefatrizine and carboxyamidotriazole, have previously been used in clinics or are undergoing clinical investigation for the treatment of cancer showing their potential as potent chemotherapy agents (Fig. 1).

Quinazoline analogues are nitrogen-containing heterocycles that exhibit a range of biological activities, including

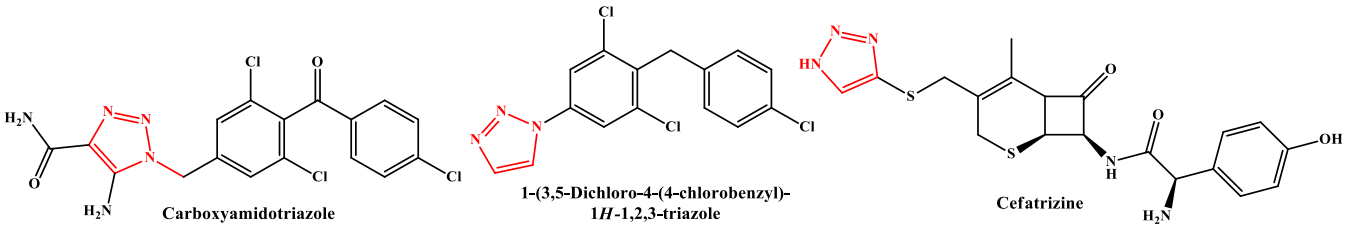

Fig. 1. Molecules containing 1,2,3-triazole hybrids under clinical trials for cancer therapy

sedative, hypnotic, antitussive, anticonvulsant, analgesic, anti-inflammatory and antihypertensive effects [17-21]. Notably, quinazoline derivatives have been found to inhibit kinase enzyme activities, thereby suppressing tumour growth. Prominently, some FDA-approved anticancer agents such as erlotinib, gefitinib, afatinib and dacomitinib incorporate the 4-aminoarylquinazoline core, a privileged scaffold extensively utilized in targeted cancer therapeutics. These agents have demonstrated clinical efficacy across multiple malignancies, including colorectal, breast, prostate and non-small cell lung cancers. The wide-ranging biomedical applications of quinazoline derivatives further underscore their pharmacological versatility [22,23] (Fig. 2).

Based on the anticancer properties of quinazoline and 1,2,3-triazole pharmacophores, a conjugate is developed using the pharmacophore hybridization approach (Fig. 3). This study aimed to design new conjugates that act as EGFR inhibitors. Moreover, *in silico* molecular docking studies is also performed on the potent conjugates identified through *in vitro* anticancer and EGFR assays [24,25].

EXPERIMENTAL

All chemicals and solvents were procured from Sigma Aldrich Company and used without any additional purification. TLC was performed on Merck silica gel 60 F_{254} precoated plates and column chromatography was carried out using silica gel (60-120 mesh). The melting points were determined with the Casia-Siamia melting point instrument (VMP-AM) and are uncorrected. ^{1}H NMR spectra were recorded on a Varian Gemini 400 MHz spectrometer and ^{13}C NMR spectra were obtained on a Bruker 100 MHz spectrometer, using DMSO as the solvent and TMS as the reference. EI (electron impact) mass spectra (at 70 eV ionising voltage) were obtained using a Shimadzu QP5050 A quadrupole-based mass spectrometer.

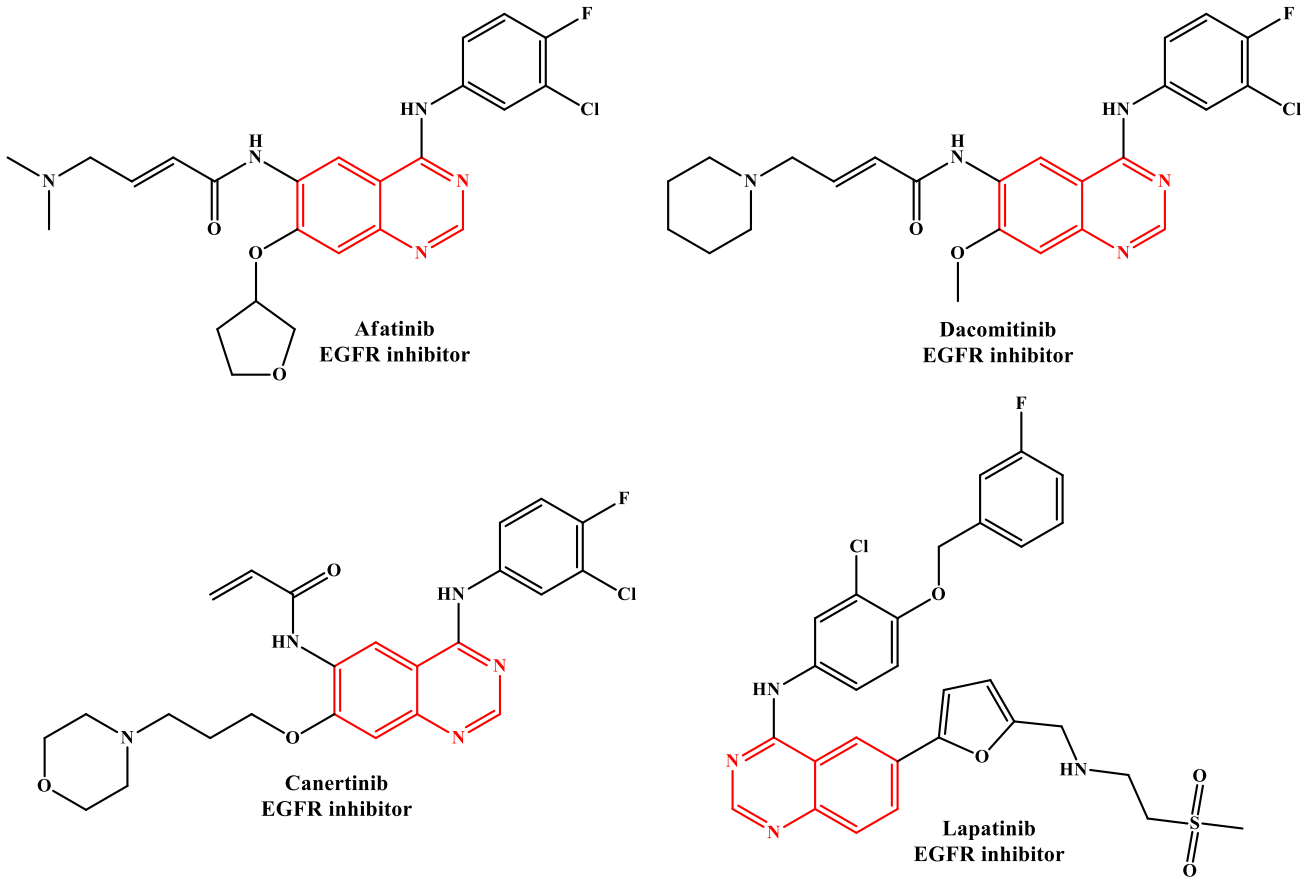

Fig. 2. Marketed anticancer drugs containing quinazoline moiety

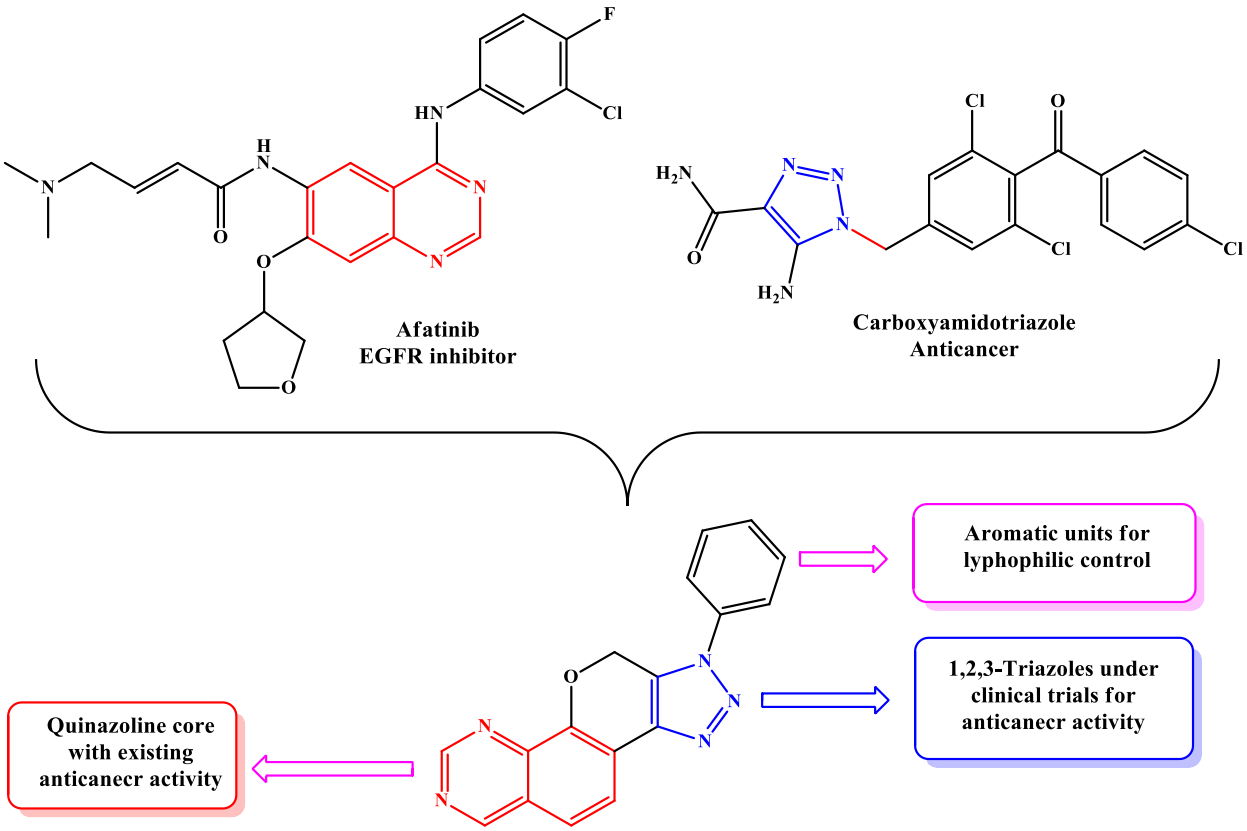

Fig. 3. Pharmacophore hybridization

Synthesis of 8-(prop-2-yn-1-yloxy) quinazoline (3): In a clean round-bottom flask, quinazolin-8-ol (0.04 mmol) dissolved in 10 mL of *N*,*N*-dimethylformamide, potassium carbonate (0.16 mmol) was added and stirred for 15 min. Then propargyl bromide (0.05 mmol) was added dropwise to the above mixture and stirred at room temperature for 10-12 h. The progress of the reaction was monitored with TLC. After completion of the reaction, the reaction mass transfers to ice-cold water. The compound was extracted with ethyl acetate and water (2 × 20 mL). The organic solvent was dried with Na_2SO_4 and brine solution. The excess solvent was removed under reduced pressure and purified by column purification with ethyl acetate and hexane in a 2:8 ratio. ^{1}H NMR (400 MHz, DMSO-d_6, δ ppm): 9.26 (s, 1H), 9.11 (s, 1H), 7.53-7.44 (m, 3H), 5.43 (s, 2H), 2.42 (s, 1H); ^{13}C NMR (100 MHz, DMSO-d_6, δ ppm): 161.8, 159.2, 158.3, 142.5, 132.6, 128.4, 124.7, 116.1, 84.4, 80.0, 60.3.

Synthesis of 8-((3-iodoprop-2-yn-1-yl)oxy)quinazoline (4): To a solution of 8-(prop-2-yn-1-yloxy) quinazoline (0.06 mL) in 10 mL of THF treated with CuI (1.2 mmol) and N-iodomorpholine (0.012 mmol), the reaction mass was stirred at room temperature for 2 h. The resulting mixture was filtered through activated neutral alumina and the filtrate was collected. The solid support was washed with chloroform (3 × 20 mL) and the collected organic layers were dried with Na_2SO_4 and brine solution. The excess solvent was removed under reduced pressure. ^{1}H NMR (400 MHz, DMSO-d_6, δ ppm): 9.26 (s, 1H), 9.16 (s, 1H), 7.59-7.45 (m, 3H), 5.49 (s, 2H); ^{13}C NMR (100 MHz, DMSO-d_6, δ ppm): 161.8, 159.5, 158.7, 142.8, 131.7, 128.7, 125.3, 116.5, 88.5, 57.5, 15.9.

General procedure for the synthesis of 1-phenyl-1,3*a*, 11,11*a*-tetrahydro-[1,2,3]triazolo[4′,5′:4,5]pyrano[3,2-*h*]-quinazoline (6a): To a solution of 8-((3-iodoprop-2-yn-1-yl)-oxy)quinazoline (0.05 mmol) in 10 mL of DMF, CuI (10 mol%) was added. Now arylazide (1.3 mmol) and *t*-BuOK (1.5 mmol) and the reaction mixture was stirred for 20-22 h at 80 ºC. The progress of the reaction was monitored with the help of TLC. After completion of the reaction, the mass was added to ice-cold water and extracted with ethyl acetate (1 × 20 mL), dried over anhydrous Na_2SO_4, filtered and concentrated under reduced pressure (**Scheme-I**). The crude products were purified by column chromatography (15% EtOAc-hexane). The other derivatives were synthesized in a similar manner.

1-Phenyl-1,11-dihydro-[1,2,3]triazolo[4′,5′:4,5]pyrano-[3,2-*h*]quinazoline (6a): Light white solid, m.p.: 186-188 ºC; ^{1}H NMR (400 MHz, DMSO-d_6, δ ppm): 9.33 (s, 1H), 9.12 (s, 1H), 7.94 (d, 1H, *J* = 5.7 Hz), 7.86 (d, 1H, *J* = 5.6 Hz), 7.26-7.38 (m, 5H), 5.60 (s, 2H); ^{13}C NMR (100 MHz, DMSO-d_6, δ ppm): 161.1, 159.3, 141.5, 140.4, 138.2, 137.3, 131.2, 130.4, 129.5, 126.3, 125.2, 123.2, 122.4, 118.4, 62.5; MS (ESI): *m/z* = 304 $[M+H]^+$; Anal. calcd. (found) % for $C_{17}H_{11}N_5O$: C, 67.77 (67.75); H, 3.68 (3.67); N, 23.24 (23.22).

1-(4-Methoxyphenyl)-1,11-dihydro-[1,2,3]triazolo[4′,5′: 4,5]pyrano[3,2-*h*]quinazoline (6b): Light white solid, m.p.: 214-214 ºC; ^{1}H NMR (400 MHz, DMSO-d_6, δ ppm): 9.26 (s, 1H), 9.10 (s, 1H), 7.81 (d, 1H, *J* = 6.2 Hz), 7.74 (d, 1H, *J* = 6.2 Hz), 7.38 (d, 2H, *J* = 5.7 Hz), 7.32 (d, 2H, *J* = 5.7 Hz), 5.63 (s, 2H), 4.02 (s, 3H); ^{13}C NMR (100 MHz, DMSO-d_6, δ ppm): 160.2, 159.6, 158.1, 141.6, 140.4, 138.2, 133.3, 131.5,

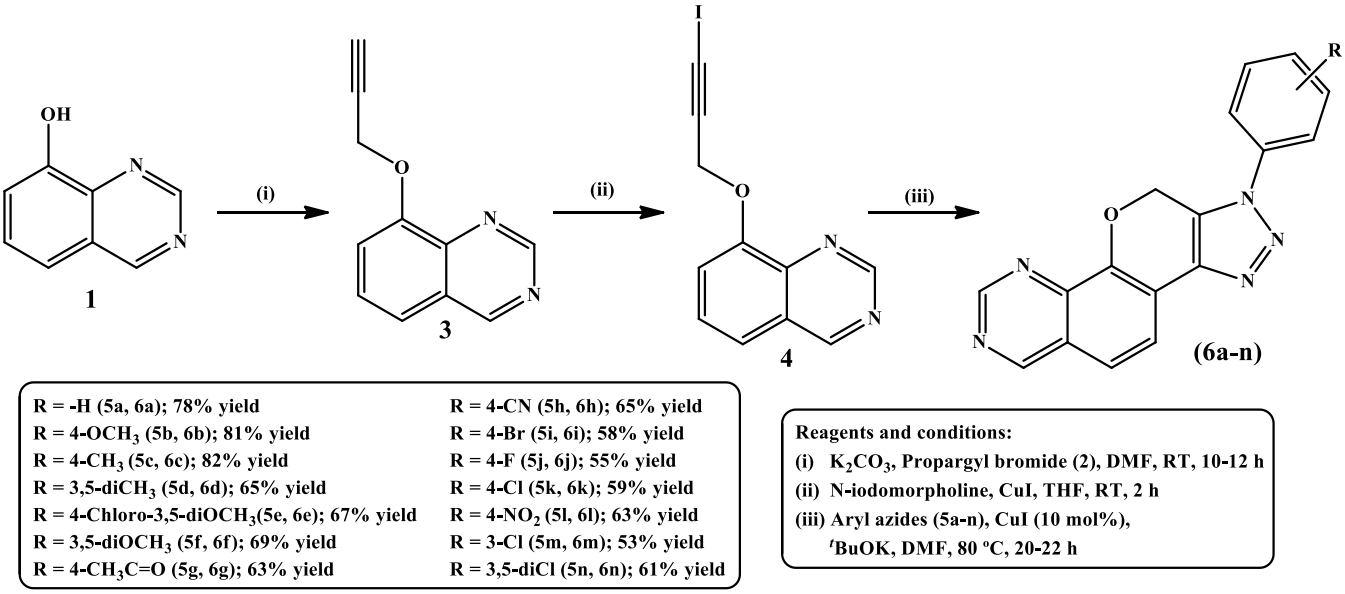

Scheme-I: Synthesis of 1,2,3-triazolo-pyrano-quinazoline conjugates (**6a-n**)

129.6, 127.3, 123.4, 122.6, 118.2, 117.3, 62.2, 58.4; MS (ESI): *m/z* = 332 $[M+H]^+$; Anal. calcd. (found) % for $C_{18}H_{13}N_5O_2$: C, 65.25 (65.24); H, 3.95 (3.94); N, 21.14 (21.12).

1-(*p*-Tolyl)-1,11-dihydro-[1,2,3]triazolo[4′,5′:4,5]pyrano-[3,2-*h*]quinazoline (6c): Light brown solid, m.p.: 196-198 ºC; ^{1}H NMR (400 MHz, DMSO-d_6, δ ppm): 9.25 (s, 1H), 9.14 (s, 1H), 7.80 (d, 1H, *J* = 5.6 Hz), 7.73 (d, 1H, *J* = 5.6 Hz), 7.61 (d, 2H, *J* = 5.2 Hz), 7.26 (d, 2H, *J* = 5.2 Hz), 5.56 (s, 2H), 2.59 (s, 3H); ^{13}C NMR (100 MHz, DMSO-d_6, δ ppm): 160.6, 158.2, 144.0, 141.8, 140.1, 139.2, 138.5, 133.4, 130.6, 127.6, 126.2, 123.5, 122.4, 118.4, 62.5, 23.5; MS (ESI): *m/z* = 316 $[M+H]^+$; Anal. calcd. (found) % for $C_{18}H_{13}N_5O$: C, 68.56 (68.54); H, 4.16 (4.15); N, 22.21 (22.20).

1-(3,5-Dimethylphenyl)-1,11-dihydro-[1,2,3]triazolo-[4',5':4,5]pyrano[3,2-*h*]quinazoline (6d): Light white solid, m.p.: 208-210 ºC; ^{1}H NMR (400 MHz, DMSO-d_6, δ ppm): 9.24 (s, 1H), 9.13 (s, 1H), 7.76 (d, 1H, *J* = 5.0 Hz), 7.65 (d, 1H, *J* = 5.1 Hz), 7.33 (s, 2H), 7.24 (s, 1H), 5.54 (s, 2H), 2.60 (s, 6H); ^{13}C NMR (100 MHz, DMSO-d_6, δ ppm): 160.4, 159.2, 144.3, 140.5, 139.1, 138.6, 137.1, 130.3, 129.4, 127.5, 126.9, 126.2, 123.4, 123.0, 118.5, 62.5, 23.4; MS (ESI): *m/z* = 330 $[M+H]^+$; Anal. calcd. (found) % for $C_{19}H_{15}N_5O$: C, 69.29 (69.27); H, 4.59 (4.58); N, 21.26 (21.25).

1-(4-Chloro-3,5-dimethoxyphenyl)-1,11-dihydro-[1,2,3]-triazolo[4′,5′:4,5]pyrano[3,2-*h*]quinazoline (6e): Light brown solid, m.p.: 196-198 ºC; ^{1}H NMR (400 MHz, DMSO-d_6, δ ppm): 9.32 (s, 1H), 9.23 (s, 1H), 7.89 (d, 1H, *J* = 6.5 Hz), 7.76 (d, 1H, *J* = 6.6 Hz), 7.63 (s, 2H), 5.70 (s, 2H), 4.11 (s, 6H); ^{13}C NMR (100 MHz, DMSO-d_6, δ ppm): 161.5, 159.3, 156.7, 141.2, 140.1, 139.5, 138.0, 130.4, 127.7, 123.4, 122.5, 119.7, 118.4, 104.5, 63.8, 59.7; MS (ESI): *m/z* = 396 $[M+H]^+$, 398 [M+2]; Anal. calcd. (found) % for $C_{19}H_{14}ClN_5O_3$: C, 57.66 (57.64); H, 3.57 (3.56); N, 17.69 (17.67).

1-(3,5-Dimethoxyphenyl)-1,11-dihydro-[1,2,3]triazolo-[4′,5′:4,5]pyrano[3,2-*h*]quinazoline (6f): Light white solid, m.p.: 228-230 ºC; ^{1}H NMR (400 MHz, DMSO-d_6, δ ppm): 9.31 (s, 1H), 9.16 (s, 1H), 7.85 (d, 1H, *J* = 5.5 Hz), 7.72 (d, 1H, *J* = 5.6 Hz), 7.34 (s, 2H), 7.22 (s, 1H), 5.56 (s, 2H), 4.08 (s, 6H); ^{13}C NMR (100 MHz, DMSO-d_6, δ ppm): 160.9, 160.1, 158.1, 141.4, 140.1, 139.1, 138.1, 130.4, 127.7, 123.4, 122.6, 118.6, 104.5, 98.2, 61.6, 59.4; MS (ESI): *m/z* = 362 $[M+H]^+$; Anal. calcd. (found) % for $C_{19}H_{15}N_5O_3$: C, 63.15 (63.14); H, 4.18 (4.17); N, 19.38 (19.36).

1-(4-([1,2,3]Triazolo[4′,5′:4,5]pyrano[3,2-*h*]quinazolin-1(11*H*)-yl)phenyl)ethan-1-one (6g): Light white solid, m.p.: 214-216 ºC; ^{1}H NMR (400 MHz, DMSO-d_6, δ ppm): 9.30 (s, 1H), 9.15 (s, 1H), 7.82 (d, 1H, *J* = 6.9 Hz), 7.72 (d, 1H, *J* = 6.9 Hz), 7.68 (d, 2H, *J* = 6.4 Hz), 7.49 (d, 2H, *J* = 6.4 Hz), 5.64 (s, 2H), 2.62 (s, 3H); ^{13}C NMR (100 MHz, DMSO-d_6, δ ppm): 198.1, 160.4, 159.2, 142.3, 141.0, 139.1, 138.2, 134.4, 130.4, 129.3, 127.5, 126.2, 123.5, 122.0, 118.4, 62.3, 29.5; MS (ESI): *m/z* = 344 $[M+H]^+$; Anal. calcd. (found) % for $C_{19}H_{13}N_5O_2$: C, 66.47 (66.46); H, 3.82 (3.80); N, 20.40 (20.38).

4-([1,2,3]Triazolo[4′,5′:4,5]pyrano[3,2-*h*]quinazolin-1(11*H*)-yl)benzonitrile (6h): Light brown solid, m.p.: 192-194 ºC; ^{1}H NMR (400 MHz, DMSO-d_6, δ ppm): 9.34 (s, 1H), 9.22 (s, 1H), 7.93 (d, 1H, *J* = 7.0 Hz), 7.81 (d, 1H, *J* = 7.1 Hz), 7.46 (d, 2H, *J* = 6.9 Hz), 7.38 (d, 2H, *J* = 6.9 Hz), 5.69 (s, 2H); ^{13}C NMR (100 MHz, DMSO-d_6, δ ppm): 161.6, 159.3, 143.5, 141.8, 138.7, 137.3, 132.4, 130.4, 127.8, 126.4, 123.5, 122.7, 121.2, 118.4, 116.5, 62.5; MS (ESI): *m/z* = 327 $[M+H]^+$; Anal. calcd. (found) % for $C_{18}H_{10}N_6O$: C, 66.25 (66.23); H, 3.09 (3.08); N, 25.75 (25.74).

1-(4-Bromophenyl)-1,11-dihydro-[1,2,3]triazolo[4′,5′:4,5]pyrano[3,2-*h*]quinazoline (6i): Light yellow solid, m.p.: 213-215 ºC; ^{1}H NMR (400 MHz, DMSO-d_6, δ ppm): 9.26 (s, 1H), 9.16 (s, 1H), 7.83 (d, 1H, *J* = 6.3 Hz), 7.74 (d, 1H, *J* = 6.2 Hz), 7.49 (d, 2H, *J* = 5.5 Hz), 7.41 (d, 2H, *J* = 5.6 Hz), 5.67 (s, 2H); ^{13}C NMR (100 MHz, DMSO-d_6, δ ppm): 160.4, 159.2, 141.0, 140.4, 138.2, 136.3, 135.4, 130.6, 127.5, 126.5, 123.2, 122.0, 121.9, 118.5, 61.5; MS (ESI): *m/z* = 380 $[M+H]^+$, 382 [M+2] ; Anal. calcd. (found) % for $C_{17}H_{10}BrN_5O$: C, 53.70 (53.69); H, 2.65 (2.64); N, 18.42 (18.40).

1-(4-Fluorophenyl)-1,11-dihydro-[1,2,3]triazolo[4′,5′:4,5]pyrano[3,2-*h*]quinazoline (6j): Light white solid, m.p.: 218-220 ºC; ^{1}H NMR (400 MHz, DMSO-d_6, δ ppm): 9.36 (s, 1H), 9.23 (s, 1H), 7.85 (d, 1H, *J* = 3.6 Hz), 7.74 (d, 1H, *J* = 3.6 Hz), 7.53 (d, 2H, *J* = 3.6 Hz), 7.44 (d, 2H, *J* = 3.6 Hz), 5.70 (s, 2H); ^{13}C NMR (100 MHz, DMSO-d_6, δ ppm): 162.1, 160.4, 159.3, 141.5, 140.1, 138.2, 134.7, 131.4, 129.4, 128.5, 123.2, 122.4, 119.4, 118.3, 62.5; MS (ESI): *m/z* = 320 $[M+H]^+$; Anal. calcd. (found) % for $C_{17}H_{10}FN_5O$: C, 63.95 (63.94); H, 3.16 (3.14); N, 21.93 (21.90).

1-(4-Chlorophenyl)-1,11-dihydro-[1,2,3]triazolo[4′,5′:4,5]pyrano[3,2-*h*]quinazoline (6k): Whitish solid, m.p.: 219-221 ºC; ^{1}H NMR (400 MHz, DMSO-d_6, δ ppm): 9.29 (s, 1H), 9.17 (s, 1H), 7.83 (d, 1H, *J* = 3.6 Hz), 7.75 (d, 1H, *J* = 3.6 Hz), 7.52 (d, 2H, *J* = 3.6 Hz), 7.43 (d, 2H, *J* = 3.6 Hz), 5.64 (s, 2H); ^{13}C NMR (100 MHz, DMSO-d_6, δ ppm): 161.7, 158.2, 144.5, 141.6, 139.2, 136.2, 135.3, 132.4, 131.4, 128.5, 126.3, 123.5, 122.3, 118.4, 62.3; MS (ESI): *m/z* = 338 $[M+H]^+$, 340 [M+2] ; Anal. calcd. (found) % for $C_{17}H_{10}ClN_5O$: C, 60.82 (60.80); H, 3.00 (2.97); N, 20.86 (20.85).

1-(4-Nitrophenyl)-1,11-dihydro-[1,2,3]triazolo[4′,5′:4,5]pyrano[3,2-*h*]quinazoline (6l): Light cream solid, m.p.: 208-210 ºC; ^{1}H NMR (400 MHz, DMSO-d_6, δ ppm): 9.35 (s, 1H), 9.25 (s, 1H), 7.96 (d, 1H, *J* = 3.6 Hz), 7.78 (d, 1H, *J* = 3.6 Hz), 7.55 (d, 2H, *J* = 3.6 Hz), 7.46 (d, 2H, *J* = 3.6 Hz), 5.71 (s, 2H); ^{13}C NMR (100 MHz, DMSO-d_6, δ ppm): 161.9, 159.3, 147.4, 143.5, 141.3, 140.1, 138.2, 131.4, 129.4, 127.5, 124.5, 123.2, 122.5, 118.4, 62.3; MS (ESI): *m/z* = 347 $[M+H]^+$; Anal. calcd. (found) % for $C_{17}H_{10}N_6O_3$: C, 58.96 (58.94); H, 2.91 (2.90); N, 24.27 (24.26).

1-(3-Chlorophenyl)-1,11-dihydro-[1,2,3]triazolo[4′,5′:4,5]pyrano[3,2-*h*]quinazoline (6m): Light yellow solid, m.p.: 225-227 ºC; ^{1}H NMR (400 MHz, DMSO-d_6, δ ppm): 9.34 (s, 1H), 9.21 (s, 1H), 7.82 (d, 1H, *J* = 3.6 Hz), 7.73 (d, 1H, *J* = 3.6 Hz), 7.59-7.46 (m, 3H), 5.65 (s, 2H); ^{13}C NMR (100 MHz, DMSO-d_6, δ ppm): 160.4, 159.2, 141.0, 139.1, 138.4, 136.7, 135.3, 132.6, 130.4, 128.7, 126.4, 125.7, 124.1, 123.2, 122.4, 118.4, 62.2; MS (ESI): *m/z* = 336 $[M+H]^+$, 338 [M+2]; Anal. calcd. (found) % for $C_{17}H_{10}ClN_5O$: C, 60.82 (60.80); H, 3.00 (2.98); N, 20.86 (20.85).

1-(3,5-Dichlorophenyl)-1,11-dihydro-[1,2,3]triazolo-[4′,5′:4,5]pyrano[3,2-*h*]quinazoline (6n): Light white solid, m.p.: 201-203 ºC; ^{1}H NMR (400 MHz, DMSO-d_6, δ ppm): 9.36 (s, 1H), 9.23 (s, 1H), 7.89 (d, 1H, *J* = 3.6 Hz), 7.80 (d, 1H, *J* = 3.6 Hz), 7.54 (d, 2H, *J* = 3.6 Hz), 7.44 (d, 2H, *J* = 3.6 Hz), 5.69 (s, 2H); ^{13}C NMR (400 MHz, DMSO-d_6, δ ppm): 161.9, 158.2, 142.5, 141.4, 139.3, 138.2, 136.4, 132.4, 127.5, 126.2, 124.3, 123.2, 122.4, 118.4, 62.5; MS (ESI): *m/z* = 370 $[M+H]^+$, 372 [M+2]; Anal. calcd. (found) % for $C_{17}H_9Cl_2N_5O$: C, 54.86 (54.85); H, 2.98 (2.96); N, 18.82 (18.80).

MTT assay: Each well of a 96-well tissue culture microtiter plate received 100 mL of full media containing 1×10^4 cells. The plates were maintained at 37 ºC in a humidified 5% CO_2 incubator for 1 h prior to the test. After the medium was withdrawn, 100 mL of fresh media containing the test compounds and erlotinib at different concentrations (0.5, 1 and 2 mM) was added to each well. We next incubated the wells at 37 ºC for 24 h. MTT dye (10 mL) were added to each well and the wells were left to incubate at 37 ºC for two more hours. The formazan crystals were dissolved in 100 μL of extraction buffer and the optical density (OD) was measured at 570 nm using a Varioskan multimode reader (Thermo-Scientific). The final DMSO concentration in the medium did not exceed 0.25%.

Tyrosine kinase EGFR inhibitory activity: The tyrosine kinase EGFR inhibitory activity study was carried out by EGFR Kinase Assay Kit (PBS Bioscience, catalogue #40321). The drug Erlotinib was used as the standard. The outcomes of the results were represented in triplicate. The IC_{50} values for the active compounds and the standard drug were calculated as the mean of three trials, with standard deviations included.

Molecular docking studies: The molecular docking investigation was conducted using Auto Dock 4.2. A protein with the PDB ID: 1MI7 is downloaded from the protein database bank. After adding polar hydrogens, the ligand and water are taken out of the protein and computed gasteiger charges. After energy minimization, the ligands are drawn using chemdraw 12 and saved as .mol files. They are subsequently transformed using Discovery Studio into a pdb file. By selecting 60 points along three coordinate axes, a grid box is produced. The dpf file was produced using the Lamarckian GA (4.2) method.

RESULTS AND DISCUSSION

The general steps for synthesized novel 1,2,3-triazolo-pyrano-quinazoline conjugates (**6a-n**) are outlined in **Scheme-I**. Initially, compound quinazolin-8-ol (**1**) was treated with propargyl bromide (**2**) in DMF solvent and K_2CO_3 was used as base and stirred under room temperature for 10-12 h, obtaining compound 8-(prop-2-yn-1-yloxy)quinazoline (**3**). Then compound **3** was treated with N-iodomorpholine in the presence of CuI in THF at room temperature for 2 h to afford the intermediate iodoalkyne. The third step involves CuI-catalyzed two cascade reactions are 1,3-dipolar cycloaddition of the iodoalkyne intermediate (**4**) and aryl azides (**5a-n**) and C-H arylation of the triazole ring to give final fused 1,2,3-triazole compounds (**6a-n**) in good yield [26].

Anticancer activity: The newly synthesized 1,2,3-triazolo-pyrano-quinazoline conjugates (**6a-n**) anticancer activity was evaluated against two human cancer cell lines such as MCF-7 and HepG-2, using the MTT assay. The test results were compared with the standard drug erlotinib and the IC_{50} values (μM) are presented in Table-1. The data indicate that compound **6e** exhibits greater potency than erlotinib, while compounds **6b**, **6d** and **6f** show activity comparable to the standard.

The structure-activity relationship (SAR) analysis highlights the influence of phenyl-ring substituents on anticancer activity. The presence of two strong electron-donating methoxy groups at the 3rd and 5th positions enhanced activity signifycantly, with compound **6e** showing superior potency (IC_{50} = 13.05 ± 0.08 μM and 9.70 ± 0.06 μM) compared to the standard drug. Strong electron-donating groups such as methoxy, regardless of their position, generally improved activity. Introducing weaker electron-donating methyl groups at the same positions (compound **6d**) resulted in moderately reduced activity, while compound **6c**, bearing only one methyl substituent, showed minimal activity. Compound **6a**, lacking any substituents, exhibited the lowest activity among the series,

TABLE-1
In vitro ANTICANCER ACTIVITY OF 1,2,3-TRIAZOLO-PYRANO-QUINAZOLINE CONJUGATES (**6a-n**) WITH IC_{50} IN μM[a]

Compound	R	[b]MCF-7	[c]HepG-2	MCF-10A[d]
6a	-H	28.25 ± 1.03	32.32 ± 0.13	ND
6b	4-OCH_3	17.05 ± 0.08	12.03 ± 0.10	98.20 ± 0.08
6c	4-CH_3	30.07 ± 0.10	25.03 ± 0.14	ND
6d	3,5-diCH_3	21.90 ± 0.05	13.75 ± 0.06	94.23 ± 0.06
6e	4-Chloro-3,5-OdiCH_3	13.05 ± 0.08	9.70 ± 0.06	96.12 ± 0.10
6f	3,5-diOCH_3	16.60 ± 0.10	14.60 ± 0.10	92.80 ± 0.17
6g	4- $COCH_3$	36.20 ± 0.52	47.30 ± 0.09	ND
6h	4–CN	21.30 ± 1.10	20.10 ± 1.02	ND
6i	4-Br	46.23 ± 0.25	48.47 ± 1.03	ND
6j	4-F	52.80 ± 0.70	60.08 ± 0.04	ND
6k	4-Cl	>100	66.10 ± 0.06	ND
6l	4-NO_2	59.20 ± 0.10	63.22 ± 0.13	ND
6m	3-Cl	68.23 ± 0.20	72.20 ± 0.21	ND
6n	3,5-diCl	72.20 ± 0.10	69.40 ± 0.05	ND
Erlotinib		15.06 ± 0.08	10.75 ± 0.30	94.10 ± 0.16

Abbreviation: ND, not determined. [a]IC_{50} after 26 h of incubation, each data represents as mean ± SD values from three different experiments performed in triplicates. [b]MCF-7: breast cancer cell line. [c] HepG-2: liver cancer cell line. [d]MCF-10A: breast healthy cell line.

confirming the beneficial role of electron-donating groups in enhancing potency.

In case of electron-withdrawing substituents, compound **6h,** containing a –CN substituent at the 4th position, was found to have good activity. The introduction of the acetyl substituent at the 4th position resulted in the compound **6g** showing slightly lower activity as compared to compound **6h**. Compounds **6i**, **6j**, **6k**, **6l**, **6m** and **6n**, with halogen substituents such as chloro, fluoro, bromo, nitro and dichloro, irrespective of their positions, display very poor activity compared to the standard drug. Lastly, the more potent compounds (**6e**, **6b** and **6f**) were tested for anticancer activity on the normal cancer cell line (MCF-10 A) and the outcomes displayed that all of them showed less cytotoxicity, complete with IC_{50} values above 98.20 μM.

***In vitro* tyrosine kinase EGFR inhibitory activity:** The tyrosine kinase EGFR inhibitory activity of the three potent compounds was evaluated. The results showed that compound **6e** exhibited higher EGFR inhibitory activity (0.93 ± 0.06 μM) compared to the standard drug erlotinib. In contrast, compounds **6b** (1.86 ± 0.07 μM), **6d** (1.89 ± 0.09 μM) and **6f** (1.52 ± 0.02 μM) displayed lower activity compared to both the standard drug and compound **6e**.

Molecular docking studies: Molecular docking studies were carried out by taking epidermal growth factor receptor (pdb id: 1M17) as the target protein. The protein was obtained from protein data bank [27]. Out of four compounds that were docked the compound **6d** having two methyl groups at 3rd and 5th positions have exhibited highest binding energy *i.e.* -9.85 kcal/mol with EGFR. The nitrogen atom of 1,2,3-triazole ring has formed a hydrogen bond with MET769 residue with bond length of 1.66 Å. Similarly, the nitrogen atom of quinazoline core has formed one hydrogen bond with LYS721 amino acid with bond length of 2.08 Å. The residues LEU694, ALA719, LEU768, MET769 and PRO770 have formed hydrophobic pocket around the ligand **6d**. Molecule **6f** having methoxy groups at 3rd and 5th positions and chlorine atom at 4th position has displayed second highest binding energy (-9.63 kcal/mol) and formed two hydrogen bonds with LYS721 and MET769 residues with bond lengths 2.06 Å and 1.66 Å, respectively. Similarly, compounds **6b** and **6e** also formed two hydrogen bonds each with same amino acids MET769 and LYS721 and their binding energies also in the same range *i.e.* -9.22 kcal/mol and -9.35 kcal/mol, respectively. Finally, the reference drug erlotinib also docked with EGFR where it has formed one hydrogen bond with MET769 amino acid with bond length 1.99 Å and it has shown less binding energy (-7.47 kcal/mol) than the four compounds (Table-2 and Fig. 4).

***In silico* pharmacokinetic profile (ADMET):** As ADMET data are valuable in drug discovery [25], the *in silico* pharmacokinetic profiles of compounds **6b**, **6d**, **6e** and **6m** were evaluated using pkCSM [28] and SwissADME [29]. The results were tabulated in Tables 3-5. According to the results all the four compounds have less water solubility *i.e.* log S parameter values are -3.021, -4.393, -3.002 and -3.009 respectively. They have exhibited positive Caco2 permeability (log

TABLE-2
MOLECULAR DOCKING RESULTS OF COMPOUNDS (**6b**, **6d**, **6e** AND **6f**) WITH EGFR ((PDB ID-1M17)

Entry	Binding energy (kcal/mol)	Inhibition constant	Number of hydrogen bonds	Residues involved in hydrogen bonding (bond length in Å)
6b	-9.22	173.79 nM	2	LYS721 (2.04), MET769 (1.65)
6d	-9.85	59.82 nM	2	LYS721 (2.08), MET769 (1.66)
6e	-9.35	138.96 nM	2	LYS721 (2.08), MET769 (1.65)
6f	-9.63	87.39 nM	2	LYS721 (2.06), MET769 (1.66)
Erlotinib	-7.47	3.34 μM	1	MET769 (1.99)

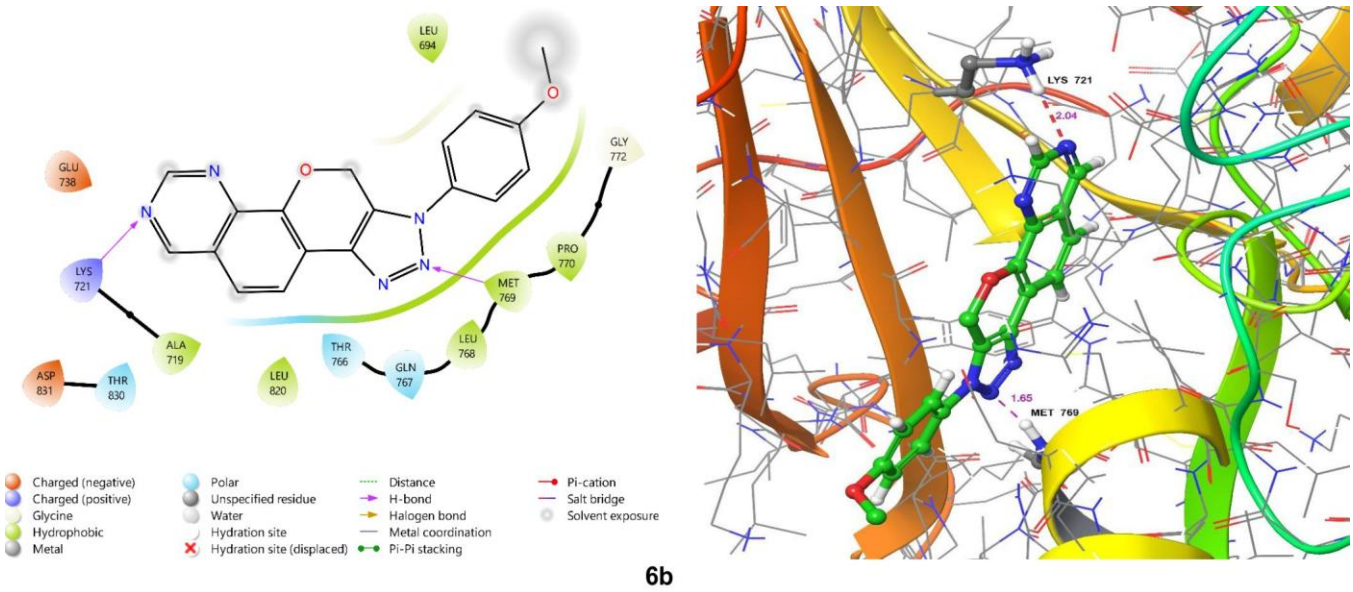
LEU 694
GLU 738
GLY 772
PRO 770
LYS 721
MET 769
ALA 719
THR 766
GLN 767
LEU 768
ASP 831
THR 830
LEU 820
LYS 721
2.04
1.65
MET 769
Charged (negative)
Charged (positive)
Glycine
Hydrophobic
Metal
Polar
Unspecified residue
Water
Hydration site
Hydration site (displaced)
Distance
H-bond
Halogen bond
Metal coordination
Pi-Pi stacking
Pi-cation
Salt bridge
Solvent exposure

6b

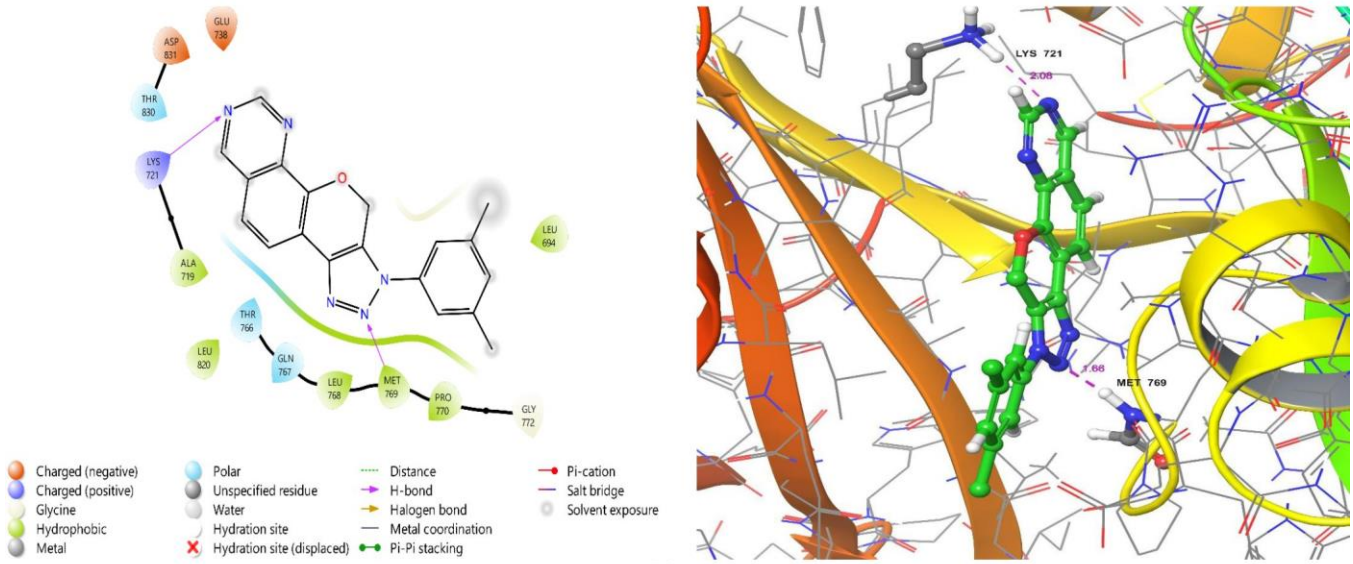
ASP 831
GLU 738
THR 830
LYS 721
ALA 719
LEU 694
THR 766
LEU 820
GLN 767
LEU 768
MET 769
PRO 770
GLY 772
LYS 721
2.08
1.68
MET 769
Charged (negative)
Charged (positive)
Glycine
Hydrophobic
Metal
Polar
Unspecified residue
Water
Hydration site
Hydration site (displaced)
Distance
H-bond
Halogen bond
Metal coordination
Pi-Pi stacking
Pi-cation
Salt bridge
Solvent exposure

6d

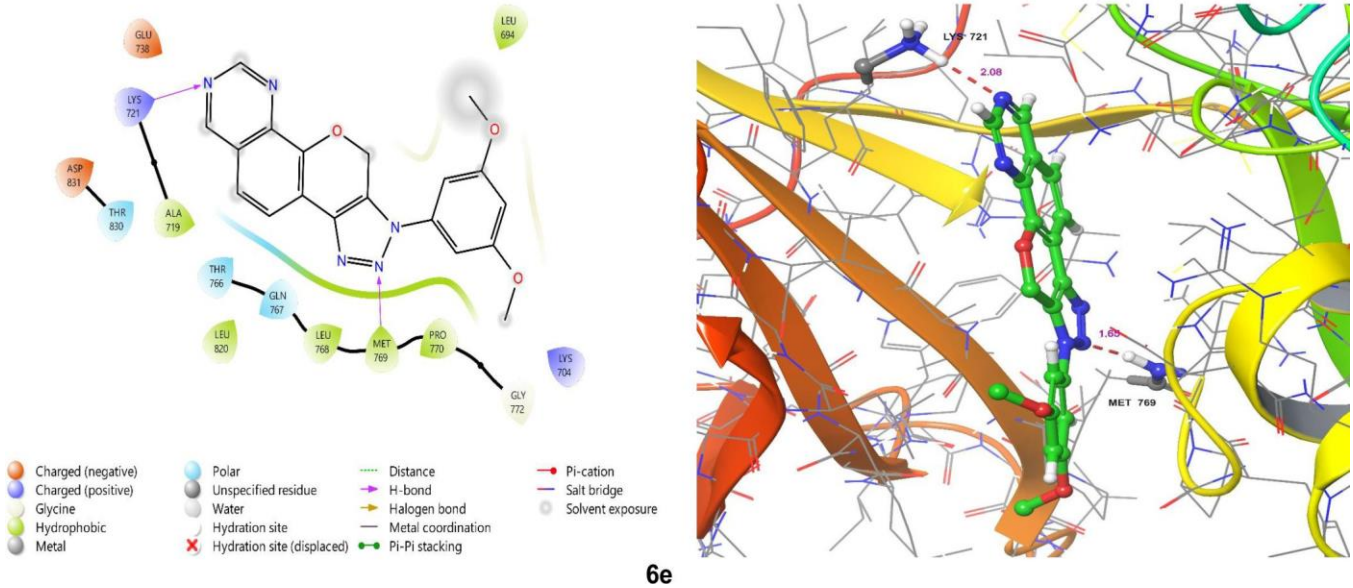
LEU 694
GLU 738
LYS 721
ASP 831
THR 830
ALA 719
THR 766
GLN 767
LEU 820
LEU 768
MET 769
PRO 770
LYS 704
GLY 772
LYS 721
2.08
1.65
MET 769
Charged (negative)
Charged (positive)
Glycine
Hydrophobic
Metal
Polar
Unspecified residue
Water
Hydration site
Hydration site (displaced)
Distance
H-bond
Halogen bond
Metal coordination
Pi-Pi stacking
Pi-cation
Salt bridge
Solvent exposure

6e

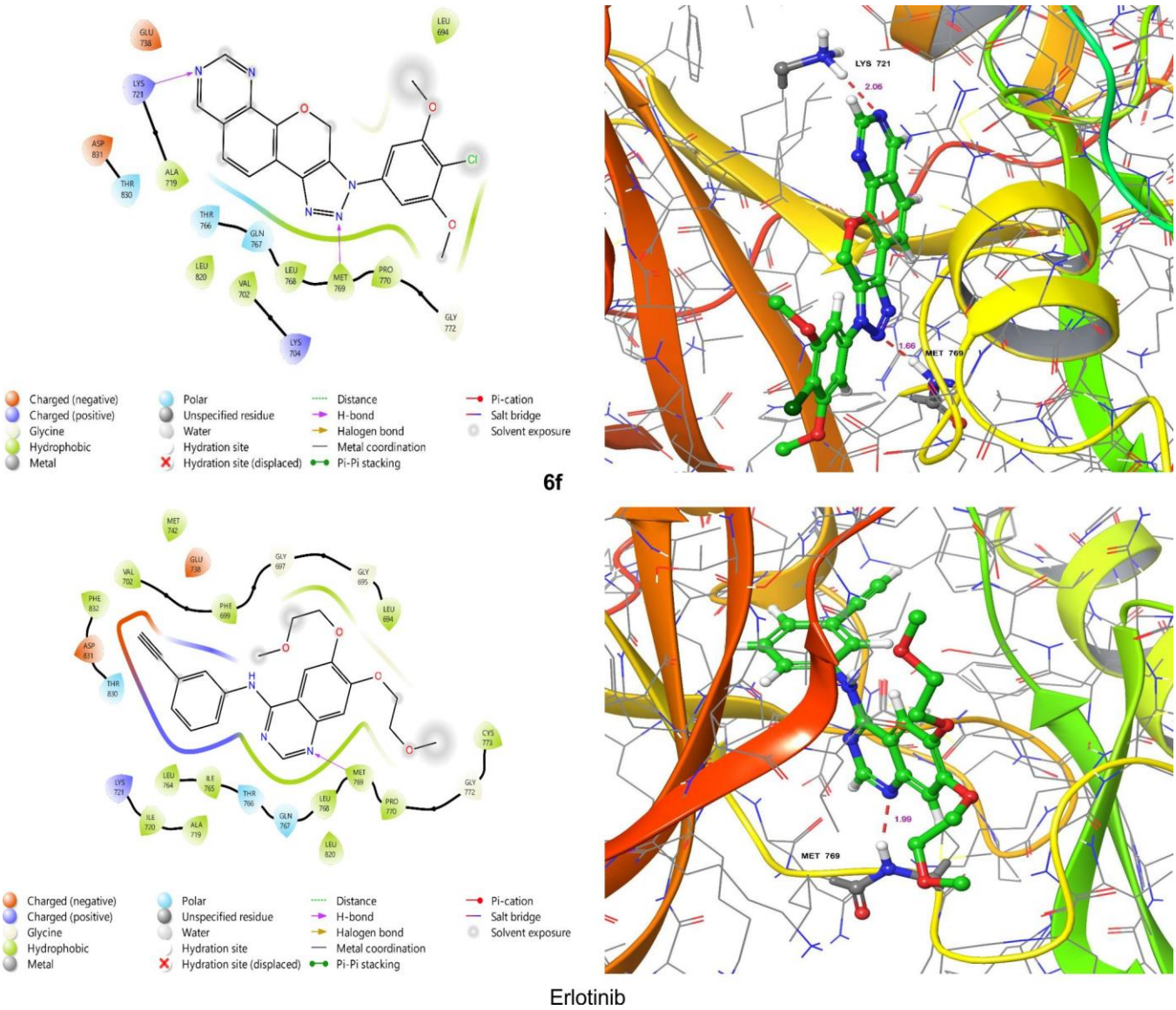

Fig. 4. 2D and 3D interaction of the compounds **6b**, **6d**, **6e**, **6f** and Erlotinib with EGFR

TABLE-3
CALCULATION OF ADME PROPERTIES OF COMPOUNDS **6b**, **6d**, **6e** AND **6f** USING pkCSM

Compd.	Absorption			Distribution				Metabolism (S = substrate; I = inhibitor)	Excretion Log (mL/min/kg)
	Log S (log mol/L)	Caco2 perm. (log Papp in 10^{-6} cm/s)	Int.abs. (% abs.)	VDss (Log L/kg)	Fract. unb. (Fu)	BBB perm. (log BB)	CNS perm. (log PS)		
6b	-3.021	1.673	100	0.116	0.239	-1.006	-3.544	CYP3A4 (S & I) CYP1A2 (I) CYP2C19 (I)	0.855
6d	-4.393	1.108	99.137	-1.027	0.094	0.003	-1.766	CYP3A4 (S) CYP1A2 (I) CYP2C19 (I)	0.613
6e	-3.002	1.802	100	-0.054	0.257	-1.228	-3.754	CYP3A4 (S & I) CYP1A2 (I)	1.034
6f	-3.353	1.427	100	-0.155	0.242	-1.208	-3.794	CYP3A4 (S & I) CYP1A2 (I)	0.919

Papp in 10^{-6} cm/s). Compounds **6b** and **6e** have 100% intestinal absorption but the compounds **6d** and **6m** have 99% intestinal absorption. Compound **6b** has positive volume of distribution (log L/kg = 0.116) and remaining three compounds have negative volume of distribution. The fraction unbound for the compounds **6b**, **6d**, **6e** and **6m** was found to be 0.239,

TABLE-4
TOXICITY PREDICTION OF COMPOUNDS **6b**, **6d**, **6e** AND **6f** USING pkCSM

Compound	AMES toxicity	hERG I inhibitor	hERG II inhibitor	Hepato toxicity	Skin permeation	Max. tolerated dose (human); log (mg/kg/day)
6b	No	No	No	Yes	No	0.709
6d	No	No	No	Yes	No	0.666
6e	Yes	No	Yes	Yes	No	0.670
6f	Yes	No	Yes	Yes	No	0.694

TABLE-5
DRUG LIKENESS AND LIPOPHILICITY PROFILE OF THE COMPOUNDS **6b**, **6d**, **6e** AND **6f** CALCULATED USING SWISSADME

Compound	Lipinski rule of 5	Ghose rule	Veber rule	Egan rule	Muegge rule	Lipophilicity (Log $P_{o/w}$)
6b	Yes	Yes	Yes	Yes	Yes	2.32
6d	Yes	Yes	Yes	Yes	Yes	2.99
6e	Yes	Yes	Yes	Yes	Yes	2.33
6f	Yes	Yes	Yes	Yes	Yes	3.22

0.094, 0.257 and 0.254, respectively. All of them were displayed negative CNS permeability (log PS) and blood-brain barrier permeability (log BB) except **6d**. All compounds interacted with CYP3A4 and inhibited CYP1A2, with **6b** and **6d** additionally inhibiting CYP2C19, while **6a**, **6c** and **6g** also showed CYP1A2 inhibition. The excretion (log value of mL/min/kg) of the compounds **6b**, **6d**, **6e** and **6m** found to be 0.855, 0.613, 1.034 and 0.636, respectively. In case of toxicity prediction, all the compounds have shown hepatotoxicity. Compound **6e** has shown AMES toxicity. None of the compounds inhibited hERG I and shown skin permeation. But compounds **6e** and **6m** have inhibited hERG II. The maximum tolerated dose (human; expressed in log value of mg/kg/day) of compounds **6b**, **6d**, **6e** and **6m** was 0.709, 0.666, 0.67 and 0.677, respectively. All the four compounds have followed Lipinski rule of five, Ghose rule, Veber rule, Egan rule and Muegge rules without any deviation. The lipophilicity (Log $P_{o/w}$) of the compounds **6b**, **6d**, **6e** and **6m** was found to be 2.32, 2.99, 2.33 and 2.81, respectively.

Conclusion

The synthesis and characterization of novel 1,2,3-triazolo-pyrano-quinazoline conjugates (**6a-n**) using well-known copper-catalyzed CuAAC and C-H arylation cascade reactions is reported. The anticancer activity of these conjugates was evaluated against two human cancer cell lines, MCF-7 and HepG-2. The results showed that conjugate **6e** exhibited more potent activity compared to the standard drug erlotinib, while compounds **6b**, **6d** and **6f** shown good activity as compared to the standard drug. The four potent compounds **6e**, **6b**, **6d** and **6f** were evaluated in a cell survival assess using the normal breast cell line MCF-10A. None of them showed significant cytotoxicity, with IC_{50} values larger than 98.20 μM. Further, the *in vitro* tyrosine kinase EGFR inhibitory of four potent compounds were evaluated and results indicate that compound **6e** exhibited higher EGFR inhibitory activity compared to the standard drug erlotinib. On the other hand, compounds **6b** and **6f** displayed lower activity compared to both the standard drug and compound **6e**. Furthermore, the molecular docking studies were also performed on four potent conjugates and the results showed that these conjugates had more EGFR-binding interactions as compared to the standard drug erlotinib. Moreover, the *in silico* pharmacokinetic profile of the potent conjugates **6e**, **6b**, **6d** and **6f** was estimated by using SWISS/ADME and pkCSM and all the four conjugates followed Lipinski, Ghose, Veber, Egan and Muegge rules without any deviation.

ACKNOWLEDGEMENTS

The authors express their gratitude to Chaitanya Deemed to be University, Department of Chemistry for supplying laboratory space.

CONFLICT OF INTEREST

The authors declare that there is no conflict of interests regarding the publication of this article.

DECLARATION OF AI-ASSISTED TECHNOLOGIES

During the preparation of this manuscript, the authors used an AI-assisted tool(s) to improve the language. The authors reviewed and edited the content and take full responsibility for the published work.

REFERENCES

1. S.H. Hassanpour and M. Dehghani, *J. Canc. Res. Pr.*, **4**, 127 (2017); https://doi.org/10.1016/j.jcrpr.2017.07.001
2. World Health Organization, Cancer (2020); https://www.who.int/news-room/fact-sheets/detail/cancer (Accessed on August 20, 2024)
3. S. Morgan, P. Grootendorst, J. Lexchin, C. Cunningham and D. Greyson, *Health Policy*, **100**, 4 (2011); https://doi.org/10.1016/j.healthpol.2010.12.002
4. L. Rong, N. Li and Z. Zhang, *J. Exp. Clin. Cancer Res.*, **41**, 142 (2022); https://doi.org/10.1186/s13046-022-02349-7
5. K. Lal and P. Yadav, *Anticancer. Agents Med. Chem.*, **18**, 21 (2018); https://doi.org/10.2174/1871520616666160811113531
6. J. Akhtar, A.A. Khan, Z. Ali, R. Haider and M.S. Yar, *Eur. J. Med. Chem.*, **125**, 143 (2017); https://doi.org/10.1016/j.ejmech.2016.09.023
7. Y. Tian, Z. Liu, J. Liu, B. Huang, D. Kang, H. Zhang, E. De Clercq, D. Daelemans, C. Pannecouque, K.-H. Lee, C.-H. Chen, P. Zhan and X. Liu, *Eur. J. Med. Chem.*, **151**, 339 (2018); https://doi.org/10.1016/j.ejmech.2018.03.059

8. H. Kaoukabi, Y. Kabri, C. Curti, M. Taourirte, J.C. Rodriguez-Ubis, R. Snoeck, G. Andrei, P. Vanelle and H.B. Lazrek, *Eur. J. Med. Chem.*, **155**, 772 (2018); https://doi.org/10.1016/j.ejmech.2018.06.028
9. B. Zhang, *Eur. J. Med. Chem.*, **168**, 357 (2019); https://doi.org/10.1016/j.ejmech.2019.02.055
10. D. Dheer, V. Singh and R. Shankar, *Bioorg. Chem.*, **71**, 30 (2017); https://doi.org/10.1016/j.bioorg.2017.01.010
11. S. Emami, E. Ghobadi, S. Saednia and S.M. Hashemi, *Eur. J. Med. Chem.*, **170**, 173 (2019); https://doi.org/10.1016/j.ejmech.2019.03.020
12. C.M. Victoria, D.M. Gabriel and S.N. Lopez, *Expert Opin. Ther. Pat.*, **27**, 415 (2017); https://doi.org/10.1080/13543776.2017.1261113
13. S. Zhang, Z. Xu, C. Gao, Q.-C. Ren, L. Chang, Z.-S. Lv and L.-S. Feng, *Eur. J. Med. Chem.*, **138**, 501 (2017); https://doi.org/10.1016/j.ejmech.2017.06.051
14. R.S. Keri, S.A. Patil, S. Budagumpi and B.M. Nagaraja, *Chem. Biol. Drug Des.*, **86**, 410 (2015); https://doi.org/10.1111/cbdd.12527
15. X.M. Chu, C. Wang, W.L. Wang, L.L. Liang, W. Liu, K.K. Gong and K.L. Sun, *Eur. J. Med. Chem.*, **166**, 206 (2019); https://doi.org/10.1016/j.ejmech.2019.01.047
16. P.N. Kalaria, S.C. Karad and D.K. Raval, *Eur. J. Med. Chem.*, **158**, 917 (2018); https://doi.org/10.1016/j.ejmech.2018.08.040
17. G. Dasari, N.S. Thirukovela, G.B. Kumar and S. Bandari, *ChemistrySelect*, **9**, e202402130 (2024); https://doi.org/10.1002/slct.202402130
18. V. Badithapuram, N. Satheesh Kumar, D. Gouthami, T. Narasimha Swamy and B. Srinivas, *ChemistrySelect*, **8**, e202204329 (2023); https://doi.org/10.1002/slct.202204329
19. R.K. Jain and V. Kashaw, *Asian J. Pharm. Pharmacol.*, **4**, 644 (2018); https://doi.org/10.31024/ajpp.2018.4.5.15
20. J. Hricovíniová, Z. Hricovíniová and K. Kozics, *Int. J. Mol. Sci.*, **22**, 610 (2021); https://doi.org/10.3390/ijms22020610
21. E. Honkanen, A. Pippuri, P. Kairisalo, P. Nore, H. Karppanen and I. Paakkari, *J. Med. Chem.*, **26**, 1433 (1983); https://doi.org/10.1021/jm00364a014
22. M.M. Ghorab, M.S. Abdel-Kader, A.S. Alqahtani and A.M. Soliman, *J. Enzyme Inhib. Med. Chem.*, **36**, 218 (2021); https://doi.org/10.1080/14756366.2020.1854243
23. S. Vilar, G. Cozza and S. Moro, *Curr. Med. Chem.*, **8**, 1555 (2008); https://doi.org/10.2174/156802608786786624
24. M.F. Zayed and M.H. Hassan, *Saudi Pharm. J.*, **22**, 157 (2014); https://doi.org/10.1016/j.jsps.2013.03.004
25. D. Zhang, G. Luo, X. Ding and C. Lu, *Acta Pharm. Sin. B*, **2**, 549 (2012); https://doi.org/10.1016/j.apsb.2012.10.004
26. S.R. Modugu, S.K. Nukala, G. Dasari, K. Bokkala and B. Srinivas, *Chem. Select*, **9**, e202404527 (2024); https://doi.org/10.1002/slct.202404527
27. J. Stamos, M.X. Sliwkowski and C. Eigenbrot, *J. Biol. Chem.*, **277**, 46265 (2002); https://doi.org/10.1074/jbc.M207135200
28. D.E.V. Pires, T.L. Blundell and D.B. Ascher, *J. Med. Chem.*, **58**, 4066 (2015); https://doi.org/10.1021/acs.jmedchem.5b00104
29. A. Daina, O. Michielin and V. Zoete, *Sci. Rep.*, **7**, 42717 (2017); https://doi.org/10.1038/srep42717